Australasian Physical & Engineering Sciences in Medicine (2019) 42:453–464
https://doi.org/10.1007/s13246-019-00740-x

SCIENTIFIC PAPER

Effects of spray parameters on skin tumour ablation volume during cryotherapy

Chandrika Kumari[1] · Amitesh Kumar[2] · Sunil Kumar Sarangi[3] · Arunachalam Thirugnanam[1]

Received: 16 May 2018 / Accepted: 20 February 2019 / Published online: 5 March 2019

Abstract

The main purpose of the study is to establish correlations for the ablation volume and the ice front as a function of the spray parameters. The ablation volume and the ice front depend upon the nozzle diameter, spraying distance and the freeze duration (spray parameters). The estimation of the ablation volume using the spray parameters shall be useful in surgical practice to ablate the different sizes of tumours. Liquid nitrogen spray cooling is carried out with 0.8 mm, 0.6 mm and 0.4 mm nozzle diameters. The spraying distance is maintained at 9 mm, 18 mm and 27 mm. The spray cooling is carried out for a single freeze–thaw cycle where freezing and thawing consist of 120 s and 130 s duration respectively. A two-dimensional heat flow equation with phase change is considered for the numerical study. The numerically calculated transient temperature (2 mm and 5 mm from the gel surface) and ice front values show confirmatory results with the experimentally measured data. Correlations are obtained to determine the ablation volume (− 50 °C and − 25 °C isothermal surfaces) and ice front (axial and lateral) with a goodness of fit ≥ 95%. The nozzle diameter has a greater impact on the ablation volume as compared to the spraying distance during 120 s of freezing. The nozzle diameter of 0.8 mm, 0.6 mm and 0.4 mm can be effectively used for cryotherapy with spraying distance up to 27 mm, 18 mm and 9 mm respectively.

Keywords Cryospray · Skin tumour · Ablation volume · Numerical simulation · Ice front

Introduction

Cryoablation is a surgical technique that uses a freezing temperature to treat skin tumours in the field of dermatology [4, 16]. This method uses a freezing agent to remove the heat from the tissue to ablate the unwanted cells. There are various freezing agents available such as ice (0 °C), ice-salt mixture (− 20 °C), freon (− 29.8 to − 40.8 °C), carbon dioxide (− 79 °C), liquid oxygen (− 183 °C) and liquid nitrogen (− 196 °C). Among these, liquid nitrogen is effective to use because of lower boiling temperature and risk-free to a human being [3]. The benign and malignant lesions are generally treated with various cryosurgical techniques such as cotton swab soaked in cryogen, carbon dioxide snow with the modulated shape, cryoprobe, copper disc and cryospray set up [36, 40]. Cryogen spray is mainly used for superficial skin tumour because it provides higher cooling efficiency at the skin surface as compared to other techniques and controlled frozen depth unlike copper disc. A plethora of work related to ablation of skin lesions or tumours using cryogen spray cooling have been reported in the literature [4, 16, 19, 34, 36, 38, 40]. From surgeons experience and practice skills, it has been found that open spray technique is suitable for a smaller size of skin tumours (≤ 20 mm in diameter and 5 mm in depth) [4]. Furthermore, it was noted that a margin (temperature should reach to − 30 °C) should be assigned across skin tumour before the commencement of cryotherapy [36].

The main task in open spray technique is to destroy an unwanted tumour and save the healthy tissue during a freeze–thaw cycle. In this procedure, intraoperative monitoring techniques are available to monitor the ice ball propagation within tissues during cryotherapy. Numerous experimental studies have used the intraoperative techniques, such

✉ Arunachalam Thirugnanam
thirugnanam.a@nitrkl.ac.in

[1] Department of Biotechnology and Medical Engineering, National Institute of Technology, Rourkela, Odisha 769008, India

[2] Department of Mechanical Engineering, Indian Institute of Technology (BHU), Varanasi 221005, India

[3] Department of Mechanical Engineering, National Institute of Technology, Rourkela, Odisha 769008, India

as ultrasound, CT scan and MRI, to visualise the ice front propagation in the skin or phase change medium [7, 34, 38]. Although, these studies helped in defining the path of ice (− 0.5 °C) in a tissue or a simple gel model, it is important to find the lethal isotherm within the ice zone. Surgeons assign the lethal isotherm of −25 °C and −50 °C for benign and malignant lesion respectively [16, 40]. It is crucial to note that lethal isotherms are difficult to monitor through non-invasive devices. However, infrared (IR) camera helps in tracking the lethal zone at the surface and IR thermography can be used to record the lethal zone at the surface during cryoprobe cooling [24]. In addition to this, thermocouples are helpful in measuring lethal depth in the skin or gel model [26, 29, 36]. Meanwhile, there are difficulties in measuring lethal temperature with thermocouples at multiple tissue locations.

Regions of lethal zone and ice zone can accurately be estimated using numerical methods for cryosurgery [10, 14, 17, 21, 27, 28]. This information is critically important for surgeons because the ablation of healthy tissue leads to unavoidable complication and cosmetic appearance. Furthermore, a limited number of numerical studies have reported the ablation volume and temperature field in the skin model using cryogen spray cooling as compared to cryoprobe technique [6, 8, 22, 25, 30–32].

The relationship between the axial and lateral ice spread has been demonstrated in the skin or tissue-like substances during the experimental study [7, 34, 38, 40] while few numerical studies have illustrated the regression analysis for lethal depth, liquidus depth and intracellular ice volume as a function of convective heat transfer coefficient for 30 s of freezing [31, 32]. However, studies that correlate the effect of spray parameters (nozzle diameter, spraying distance and freeze duration) on the ice front and ablation volume during open spray technique are rare.

In order to address the problem, this study proposes a correlation of ice front (axial and radial) and ablation volume (−50 °C and −25 °C isothermal surfaces) in a tissue-mimicking gel as a function of nozzle diameter, spraying distance and freeze duration. Furthermore, the influence of these parameters on necrotic volume and ice front propagation in the gel phantom are studied during cryotherapy for the application of superficial skin tumour ablation.

Materials and methods

Experimental setup

Figure 1 depicts the experimental setup for the liquid nitrogen spray cooling on a tissue-mimicking gel. 0.6% (w/v) of agarose gel is used as a gel phantom during cryotherapy. The initial temperature of gel phantom is 24 °C to

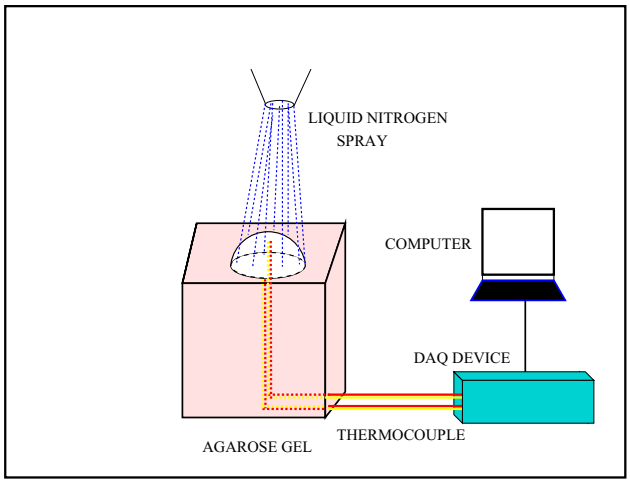

Fig. 1 Schematic representation of the liquid nitrogen spray cooling on gel phantom

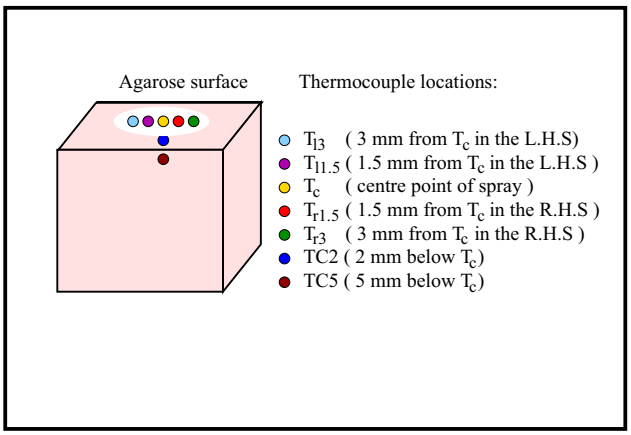

Fig. 2 Thermocouple locations in the lateral and axial directions in a tissue-mimicking gel

maintain the integrity of gel while the ideal temperature of the human skin is around 34 °C to 37 °C. The liquid nitrogen spray cooling is carried out with cryogen spray setup (SMTPraha, CS-1, Czech Republic) with 0.8 mm, 0.6 mm and 0.4 mm nozzle diameters. The distances from the nozzle to gel surface (z) were set to be 9 mm, 18 mm and 27 mm. The spray cooling was carried out for a single freeze–thaw cycle, where freezing and thawing consist of 120 s and 130 s cycles respectively. The K type thermocouples were used to record the temperature at different axial and radial locations as shown in Fig. 2. The accuracy in the temperature measurement using K type thermocouple is ±2 °C. The data acquisition (DAQ) device (National Instruments, USB 9213, US) is attached to thermocouples to acquire the temperature with the help of Lab View 2013 software in °C.

Table 1 The value of constant a and T_{min} for predicting T_{sur}

N_d (mm)	0.8			0.6			0.4		
z (mm)	9	18	27	9	18	27	9	18	27
a	6	4.5	3.5	3.5	2.8	1.8	2.6	1.5	1.3
T_{min} (°C)	− 183	− 181	− 176	− 155	− 145	− 130	− 70	− 60	− 25

N_d: nozzle diameter

The transient temperature is measured in radial and axial directions for 120 s freezing and 130 s thawing cycles. Each set of experiment was conducted in triplicate to obtain accurate results. The average temperature has been calculated from three trials, and the standard deviation for the experimental data has been represented by error bar. The temperature data has an overall uncertainty of ±8 °C for the three times measured temperature for all the cases. The ice front propagation in the lateral and axial directions for 120 s cycle of freezing is captured using a digital camera Nikon COOLPIX L27. The data of the ice front have been measured with Image J software where the accuracy in the measurement is 0.4 mm. Also, the experimentally measured ice front in triplicate has an uncertainty of 0.8 mm.

Approximation of surface boundary condition

Figure 3a, b and c show the transient temperature at the gel surface during 120 s freezing cycle with nozzle diameters of 0.8 mm, 0.6 mm and 0.4 mm for a spraying distance of 18 mm. The symbols with error bar represent the experimental values, and a solid line curve shows the best curve fit obtained from the experimental data (T_{sur}). It is observed that the temperature obtained at various locations decreases continuously during the freezing duration. In Fig. 3 fluctuations in the temperature field have been observed during 120 s of freezing due to liquid nitrogen disintegration into spurts while leaving the nozzle. The temperature obtained at $T_{r1.5}$ and T_{r3} locations are similar with $T_{l1.5}$ and T_{l3} locations respectively. This shows that ice front propagates radially and axially in a symmetrical manner; hence, an axisymmetric two-dimensional model has been used for the numerical study. The cryogen spray zone for 0.8 mm, 0.6 mm and 0.4 mm nozzle diameter were approximated as 3 mm, 2 mm and 1.1 mm respectively. The approximation is based on the lesser temperature gradient within the specified cryogen spray zone. A similar observation has been made for other cases of $z = 9$ mm and 27 mm. The general expression for the best curve fit to calculate T_{sur} is given below; T_{sur} is used as a boundary condition at the cryogen spray zone for 120 s of freezing,

$$T_{sur} = T_{min} + (T_i - T_{min}) \exp\left(\frac{-a \cdot t}{120}\right) \tag{1}$$

where a is the value of coefficient used for calculating T_{sur}, t is time, T_i is initial temperature and T_{min} is the lowest temperature observed at the gel surface. This equation is calculated using R software with the method of least squares. The value of a and T_{min} are enlisted in Table 1 for 0.8 mm, 0.6 mm and 0.4 mm nozzle diameter with three different spraying distance of $z = 9$ mm, 18 mm and 27 mm for each nozzle. The present estimated surface temperature T_{sur} within the cryogen spray zone provides an accurate boundary condition for the modelling of skin cryotherapy using spray cooling.

Mathematical formulation

A heat flow equation with phase change [9, 37] is considered for the numerical study. This equation is given as follows:

$$\frac{\partial(\rho H)}{\partial t} = \nabla \cdot (k \nabla T) \tag{2}$$

$$H = h + h_{\text{lat}} \tag{3}$$

$$h = cdT \tag{4}$$

$$h_{\text{lat}} = Ldg \tag{5}$$

where H is total enthalpy, h_{lat} is latent heat, h is sensible heat, c is specific heat, L is latent heat of fusion, g is liquid fraction and T is the temperature of gel domain. Then the final equation which is used to solve the temperature field in the whole domain is

$$\rho c \frac{\partial T}{\partial t} = \nabla \cdot (k \nabla T) - \rho L \frac{\partial g}{\partial t} \tag{6}$$

where the value of g is estimated using [37]

$$\text{Frozen region} : g = 0.0 \tag{7}$$

$$\text{Mushy region} : g = \frac{T - Ts}{T_l - Ts} \tag{8}$$

$$\text{Unfrozen region} : g = 1.0 \tag{9}$$

where l and s denote the liquidus and solidus region respectively. The mushy region in the gel domain lies in the temperature range of −1 °C and 0 °C. The thermal properties such as density (ρ), specific heat (c) and thermal conductivity (k) during phase change are determined as [37].

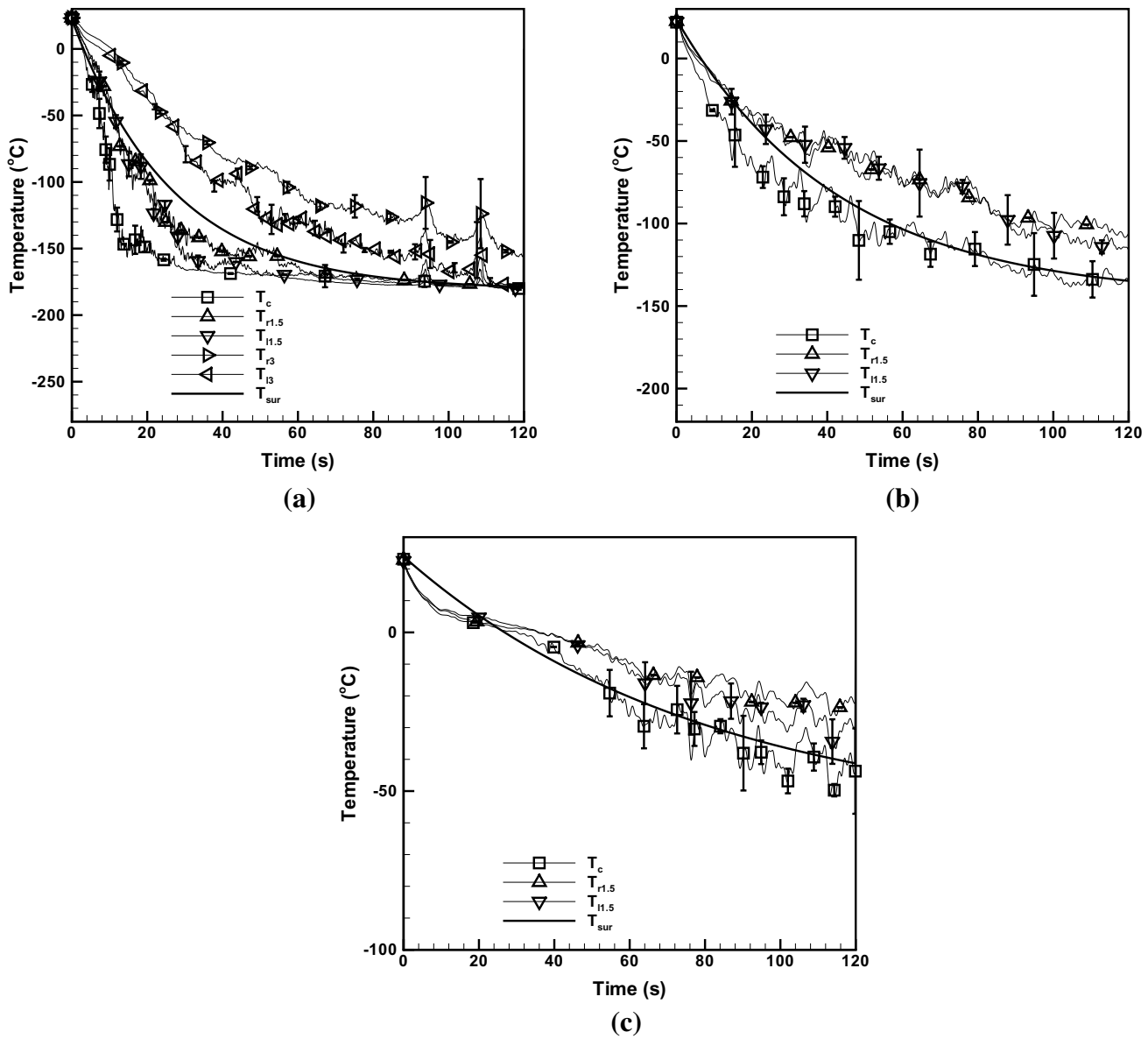

Fig. 3 Surface temperature obtained at the spray zone using 0.8 mm, 0.6 mm and 0.4 mm nozzle diameter for $z = 18$ mm. **a** Nozzle diameter: 0.8 mm, **b** nozzle diameter: 0.6 mm and **c** nozzle diameter: 0.4 mm

$$\text{for } T_s < T < T_l : c = gc_l + (1-g)c_s \tag{10}$$

$$\text{for } T_s < T < T_l : k = gk_l + (1-g)k_s \tag{11}$$

$$\text{for } T_s < T < T_l : \rho = g\rho_l + (1-g)\rho_s \tag{12}$$

The final Eq. (6) remains the same during a single freeze–thaw cycle; the thermal properties are going to vary depending upon the phase change region in the gel domain. The experiment was performed on a tissue-mimicking gel and hence, the metabolic heat generation and blood perfusion are not considered in the present study. The average depth of a skin tumour is 1.8 mm [15], which majorly cover the dermis part of the skin. Thus, 0.6% (w/v) agarose gel is used to mimic the tissue because its thermal properties are comparable with water [28] and dermis layer of skin [12, 31]. The properties of the gel used for solving the numerical equation are obtained from previous studies [18, 33]. The thermal conductivity and specific heat of tissue-mimicking gel are assumed as temperature dependent properties.

A two-dimensional axisymmetric cylindrical domain was used for the formulation such that axial and radial domains have dimensions of 70 mm each. The structured orthogonal grid is considered for the numerical domain and solved with finite volume method [13, 17]. The implicit three time level

method with time increment of $\nabla t = 0.01$ s is used to solve the unsteady part while central difference scheme is used to discretise the diffusive part for solving the numerical Eq. (6). The initial and boundary conditions for the numerical study is shown in Fig. 4. The upper surface of gel domain is divided into two zones, i.e., cryogen spray and convective region during 120 s of freezing. The T_{sur} is assumed across the cryogen spray zone, while convective heat transfer coefficient, $h = 10\,\mathrm{W/m^2K}$, is applied in the convective region during freezing [31]. Within 130 s of thawing, the convective heat transfer coefficient is assumed at the upper surface of gel.

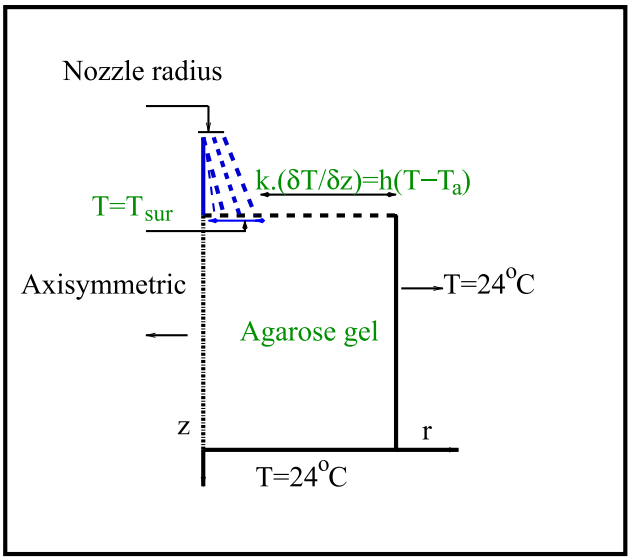

Fig. 4 Initial and boundary conditions of the computational domain

Results

The transient temperature and ice front propagation were measured experimentally in an in-vitro study during cryotherapy. The liquid nitrogen spray cooling on the gel surface has been carried out with nozzle diameters of 0.8 mm, 0.6 mm and 0.4 mm. Also, the spraying distance from the nozzle to the target site has been maintained as 9 mm, 18 mm and 27 mm. The freeze–thaw cycle during cryofreezing procedure consists of 120 s freezing and 130 s thawing. In this numerical formulation, heat flow equation with phase change is solved on a two-dimensional axisymmetric orthogonal grid with finite volume method. The numerically calculated data were verified with the experimentally measured data for an in-vitro study. The ablation volume is predicted numerically; this information is useful for the surgeon in order to properly manage cryotherapy procedures. Furthermore, this study has proposed unique dependence of ablation volume and ice front on freeze duration (t), nozzle diameter (N_d) and distance from the nozzle to the gel surface (z).

Validation of predicted results with measured data

Temperature distribution

Figure 5a and b represent the transient temperature in the axial direction at 2 mm and 5 mm locations from the gel surface for $z = 18$ mm. The result shows the temperature profiles for 0.8 mm, 0.6 mm and 0.4 mm nozzle diameters for 120 s freezing and 130 s passive thawing. The temperature field decreases gradually during freezing, while the temperature suddenly rises from an end temperature to 0 °C during initiation of thawing. This temperature remains constant for further thaw duration. The end temperature (T_{min}) obtained at TC2 location with 0.8 mm, 0.6 mm and 0.4 mm nozzle diameters for $z = 18$ mm is −138 °C, −68 °C and −8 °C respectively while at TC5 location it is −66 °C, −4 °C and 8 °C respectively. Hence, it has been observed that the lethal temperature is obtained up to 2 mm depth from gel surface with 0.6 mm nozzle diameter while it is 5 mm depth from gel surface with 0.8 mm nozzle diameter. A similar observation of temperature drop has been made with 0.8 mm, 0.6 mm and 0.4 mm nozzle diameter for $z = 9$ mm and 27 mm. The numerical results are verified with experimental results as shown in Fig. 5. The temperature difference of ±8 °C is observed between experimentally measured and numerically calculated results for all the cases. This change is significant in physiological term but the imaging of freezing front from ultrasound leads to uncertainty of 1 mm (10–15 °C) as reported in the earlier study [28] and hence, this error is acceptable during cryofreezing.

Icefront

Figure 6a and b demonstrated the experimentally and numerically measured axial and radial ice fronts for $z = 18$ mm during liquid nitrogen spray. In a similar way, ice propagates for 0.8 mm, 0.6 mm and 0.4 mm nozzle diameter with spraying distance of 27 mm and 9 mm as represented in Table 2. The maximum and minimum ice front difference between experiment and simulated data are 0.2 mm and 3 mm respectively. From this, it can be stated that the average differences between the experimentally measured and numerically calculated results are 1.6 mm. The uncertainty of 1 mm is acceptable during cryofreezing as mentioned in the above section while the average difference of 1.6 mm is nearly similar to this value. The ice front generally forms in a symmetrical manner for all the cases but few cases are shown in Fig. 7a and b.

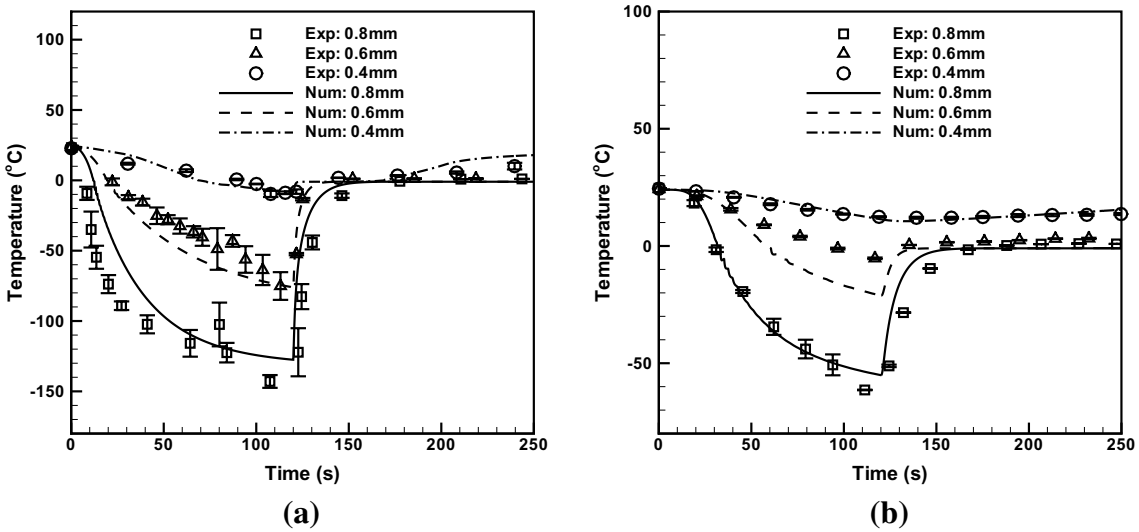

Fig. 5 Transient temperature in the axial direction during a freeze–thaw cycle. **a** 2 mm from the T_c location: $z = 18$ mm and **b** 5 mm from the T_c location: $z = 18$ mm

Correlation for ablation volume and ice front

The correlation for necrotic volume (V_n) enclosed by the −25 °C and −50 °C isothermal surfaces are obtained using the least squares method; where −25 °C and −50 °C represent the lethal isotherm for benign and malignant lesion respectively [16, 40]. The value of the coefficients are presented in Table 3.

$$V_n = (A + BN_d^2 + Cz^2)t^D z^E N_d^F \tag{13}$$

The calculated value of ablation volume from correlation is shown in Fig. 8a and b for 0.8 mm and 0.6 mm nozzle diameters. The ablation volume enclosed by −50 °C and −25 °C isothermal surface have the R^2 value of 99% between the numerically evaluated and the correlated values.

From these results, experimentally measured radial and axial ice fronts have been correlated during 120 s of freezing. The ice front gives an idea of the spread of ice ball in both lateral and axial directions. The expression for correlation of the ice front (I) is given in Eq. (14)

$$I = (Az^B)t^{0.5}N_d^C \tag{14}$$

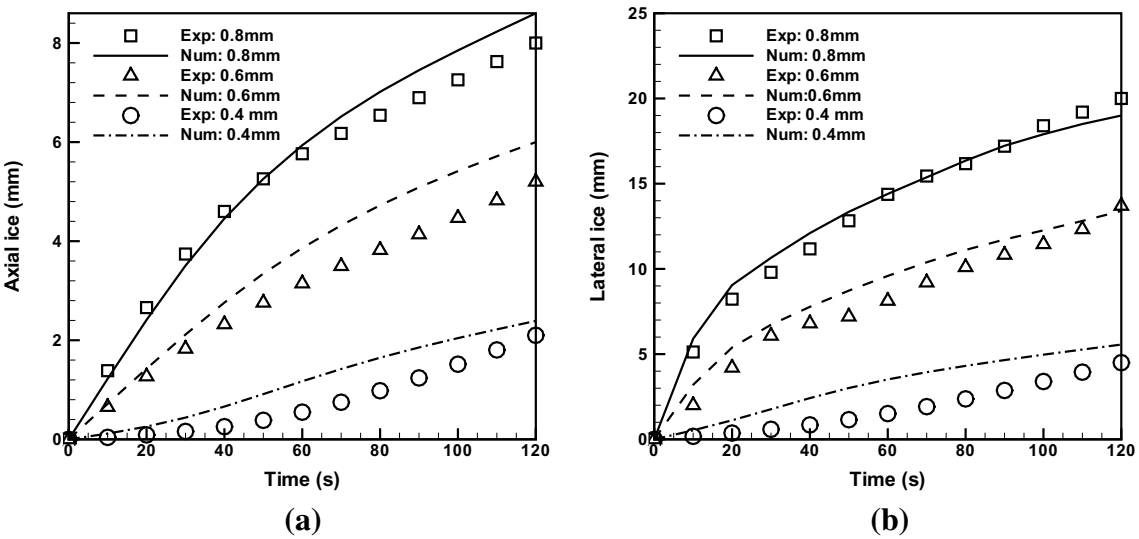

Fig. 6 The lateral and axial ice front measured during 120 s of freezing. **a** Axial ice front: $z = 18$ mm and **b** lateral ice front: $z = 18$ mm

The lateral and axial ice fronts obtained from correlation is shown in Fig. 9a–d. The R^2 value for the lateral and axial ice front are 97% and 95% respectively between the experimentally measured and the correlated data.

Figure 10 represents the − 50 °C, − 25 °C and 0 °C isotherms in a gel model at 120 s of cryogen spray using 0.8 mm, 0.6 mm and 0.4 mm nozzle diameters for $z = 27$ mm, 18 mm and 9 mm.

Discussion

Liquid nitrogen spray cooling is an effective method to treat skin tumours and the efficiency of cryoablation technique depends upon the spray parameters used by the surgeon. The spray parameters during a liquid nitrogen spray cooling technique affect the lethal and ice front propagation in the skin tissue/phase change medium. In the present study, the influence of liquid nitrogen spray cooling is studied by varying the nozzle diameter (0.8 mm, 0.6 mm and 0.4 mm)

Table 2 Experimental and numerical values of ice front at various freeze duration (Axi: axial ice front; Lat: lateral ice front; Exp: experimental; Num: numerical)

Nozzle diameter (mm)	Spraying Distance	60 s freezing				120 s freezing			
		Exp		Num		Exp		Num	
		Axi	Lat	Axi	Lat	Axi	Lat	Axi	Lat
0.8	27	6.0	13.6	5.5	13.0	7.2	20.0	8.1	18.0
	18	6.1	14.4	6.0	14.4	8.0	20.5	8.6	19.0
	9	6.3	15.1	6.4	14.8	8.1	21.0	8.9	19.2
0.6	27	2.2	6.4	3.4	8.2	4.1	12.3	5.4	11.6
	18	3.2	8.1	4.0	9.6	5.2	13.0	6.0	13.4
	9	3.8	9.1	4.5	10.2	5.3	13.7	6.6	14.0
0.4	27	0.0	0.0	0.0	0.0	0.0	0.0	1.1	3.2
	18	0.0	0.4	1.2	3.6	2.1	4.5	2.3	5.5
	9	2.2	4.8	2.0	4.8	3.0	7.0	3.2	6.8

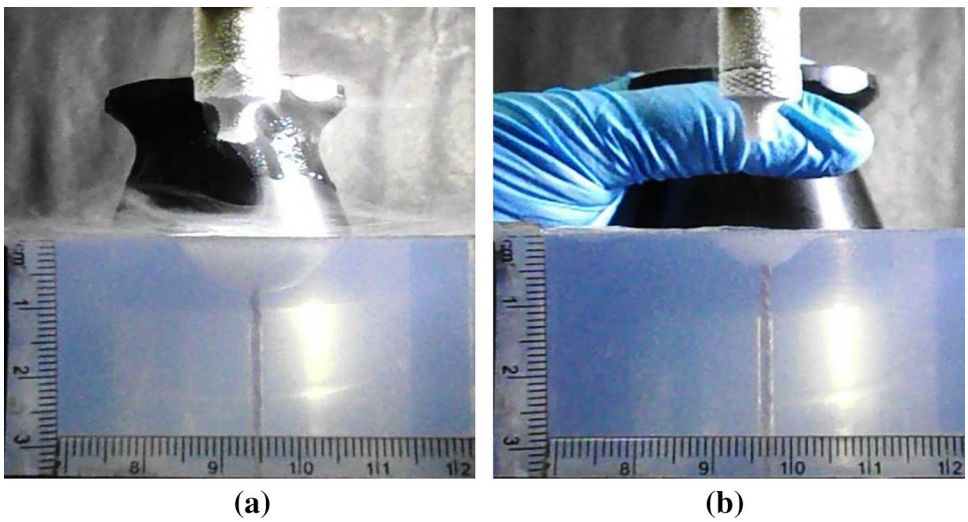

Fig. 7 Symmetrical formation of ice ball at 120 s freezing. **a** 0.8 mm nozzle diameter: $z = 18$ mm and **b** 0.6 mm nozzle diameter: $z = 18$ mm

Table 3 The value of coefficients for predicting ablation volume and ice front

Coefficient (°C)	*A*	*B*	*C*	*D*	*E*	*F*
− 25	− 80.219	396.276	− 0.055	1.035	− 0.067	1.022
− 50	− 42.258	214.37	− 0.033	0.858	− 0.061	1.879
Axial 0	1.9	− 0.163	2.115			
Radial 0	3.59	− 0.083	1.903			

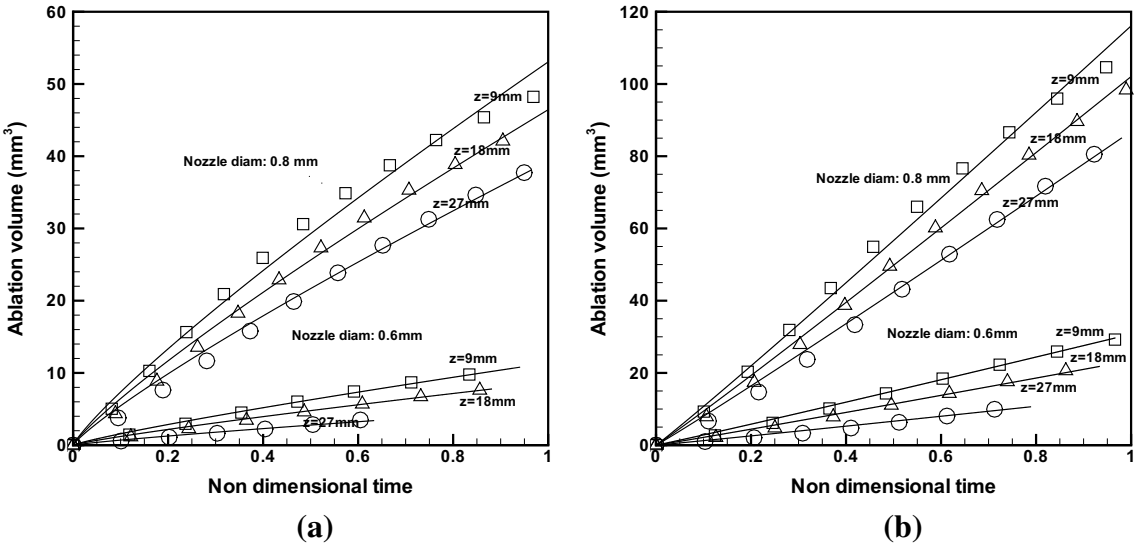

Fig. 8 Correlation obtained for ablation volume with respect to non dimensional time; symbols represent the numerical ablation volume and solid line represents the correlation values obtained from Eq. (13). **a** – 50 °C Isothermal surface and **b** – 25 °C isothermal surface

and spraying distance (27 mm, 18 mm and 9 mm) for 120 s of freezing and 130 s of thawing. The transient temperature history (2 mm and 5 mm depth from the skin surface) and ice front (axial and radial directions) obtained from the experimental study were validated numerically for various spray parameters as shown in Figs. 5 and 6 respectively. From the Fig. 5, it is apparent that the numerically predicted data are nearly similar to the experimentally recorded data. The highest discrepancies are observed for 0.6 mm and 0.8 mm nozzle diameters during 120 s cycle of freezing at 2 mm depth location and the same is observed for 0.6 mm nozzle diameter at 5 mm depth location in the gel model. The average differences between the numerically predicted and experimentally measured results are found to be ±8 °C. The difference between the simulated and measured data may be attributed to the assumed boundary conditions within the cryogen spray zone and experimental errors. During thawing the numerically predicted data adhere closely to the experimentally measured data and the major differences between these results are found for 0.8 mm nozzle diameter (2 mm and 5 mm depth locations) and 0.6 mm nozzle diameter (5 mm depth location). The reason for this difference may be due to the assumed convective heat transfer coefficient from the literature [31]. The numerically evaluated and experimentally measured ice front data are compared in Fig. 6. The axial ice front data obtained using numerical model shows good agreement with the experimentally measured data till 60 s of freezing whereas it matches till 120 of freezing for the lateral ice front. The similar observations are not found for 0.6 mm and 0.4 mm nozzle diameters. The average discrepancies between the simulated and recorded data are 1.6 mm. These discrepancies may be due to the assumed boundary condition during freezing. These values only provide the guideline or idea to the surgeons which will be helpful during the selection of the spray parameters. Similarly, the validation studies have been represented for the cryoablation technique [5, 6, 11, 14, 19, 25, 28]. The transient temperature continuously decreases for 120 s of freezing cycle with all the nozzle diameter except with 0.4 mm during liquid nitrogen spray. During initiation of thawing, the temperature remains at sub-zero temperature for a short duration and this leads to increment in the ice front propagation. However, the propagation of ice front will be lesser in such a short span of time as compared to the continuous spurts duration of liquid nitrogen. In the previous study, it is reported that the heat skin occurs at a higher rate during freezing cycle as compared to the residence time (after freezing when cryogen stays for certain duration) [35]. The present study has been carried out on an axisymmetric cylindrical domain and previously, a few authors also analysed the cryotherapy technique using axisymmetric numerical models [20, 23, 32]. During liquid nitrogen spray cooling in the present study, a symmetric ice ball formation occurred within the gel phantom as shown in Fig. 7 and hence, the data obtained from this study can be used for regular or symmetric tumour geometry.

To the best of the author's knowledge, this is for the first time that the correlations are determined for ablation volume and ice front as a function of nozzle diameter, spraying distance and freeze duration. Eqs. (13) and (14) give the correlation for ablation volume and ice front respectively for 120 s of freezing. In a related study, Torre [34] has presented a correlation between lateral and axial spread of ice in a phase change medium. They found

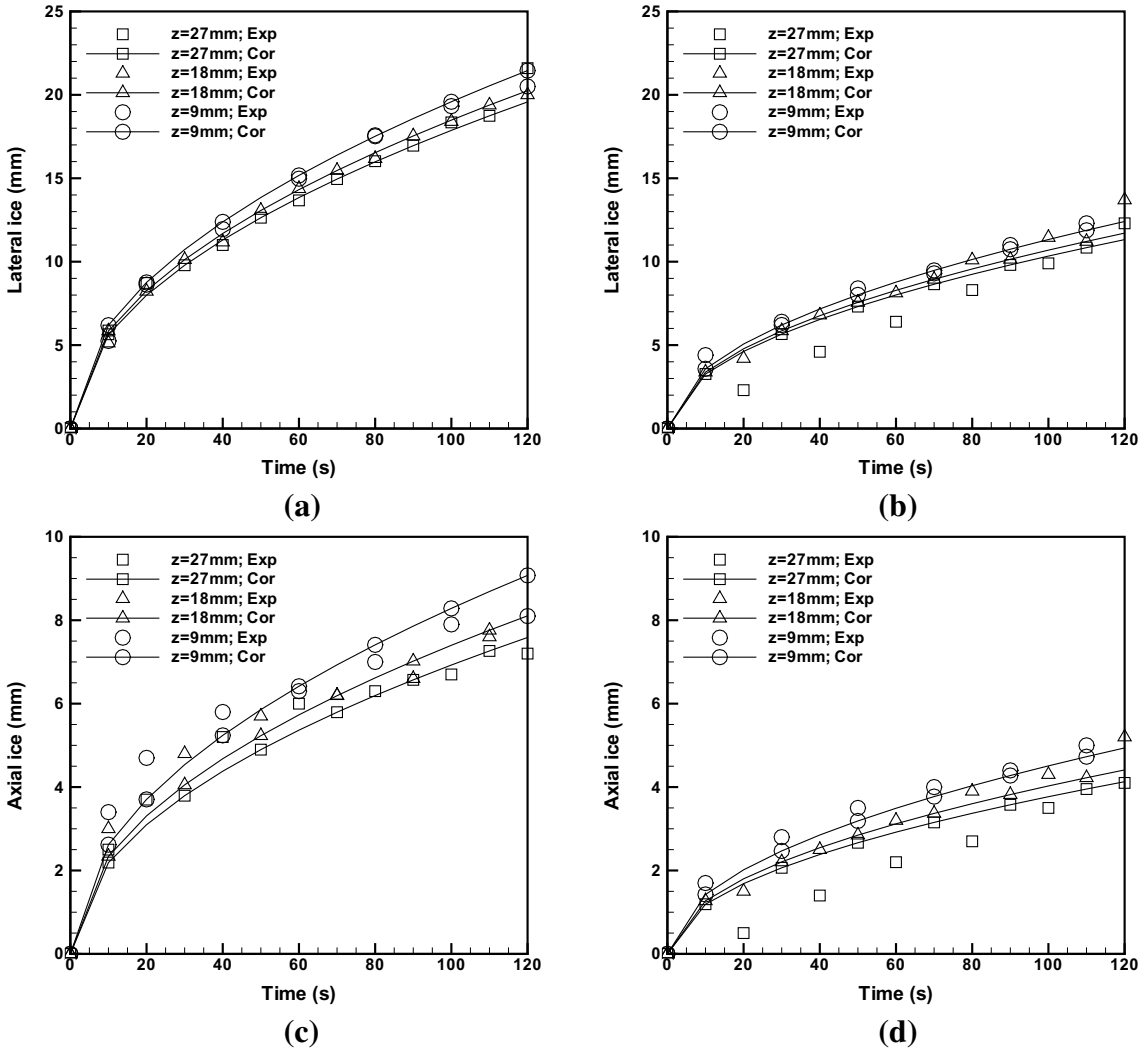

Fig. 9 Correlation obtained for lateral and axial ice front with respect to time; symbols represent the experimentally measured ice front and solid line represents the correlation values obtained from Eq. (14). **a** Lateral ice front; nozzle diameter: 0.8 mm, **b** lateral ice front; nozzle diameter: 0.6 mm, **c** axial ice front; nozzle diameter: 0.8 mm and **d** axial ice front; nozzle diameter: 0.6 mm

out that the lateral spread of ice is 1.3 times that of axial spread of ice. Meanwhile, similar result is not observed in the current case because cone spray technique was used in the reported study. In another study, it has been demonstrated that the axial spread of ice is 0.5 times of lateral spread of ice during open spray technique [40]. However, in the current study, it has been found that axial spread of ice does not satisfy the same correlation but rather depends on the nozzle diameter, spraying distance and freeze duration.

From Fig. 8, it is observed that the propagation of ablation volume represented by the −25 °C isothermal surface is approximately double of the −50 °C isothermal surface. The final ablation volume obtained by −50 °C isothermal surface with 0.6 mm nozzle diameter for spraying distance of 9 mm, 18 mm and 27 mm is 79%, 82% and 92% smaller than 0.8 mm nozzle diameter respectively. The rate of ablation volume obtained with nozzle diameter of 0.8 mm and spraying distance of 27 mm is substantially larger than that of nozzle diameter of 0.6 mm and spraying distance of 9 mm; even though the former has a higher spraying distance as compared to the latter. From these results, we could summarise that the effect of nozzle diameter is larger on ablation volume as compared to the distance from the nozzle to gel surface.

The spraying distance is optimised with nozzle diameter, which can provide a better approach to surgeons for skin tumour ablation during cryotherapy. In Fig. 8, it is observed that the ablation volume significantly increases with increase in nozzle diameter and decrease in spraying distance. With the increase in spraying distance, the rate of evaporation increases and it decreases the efficiency of cryogen spray

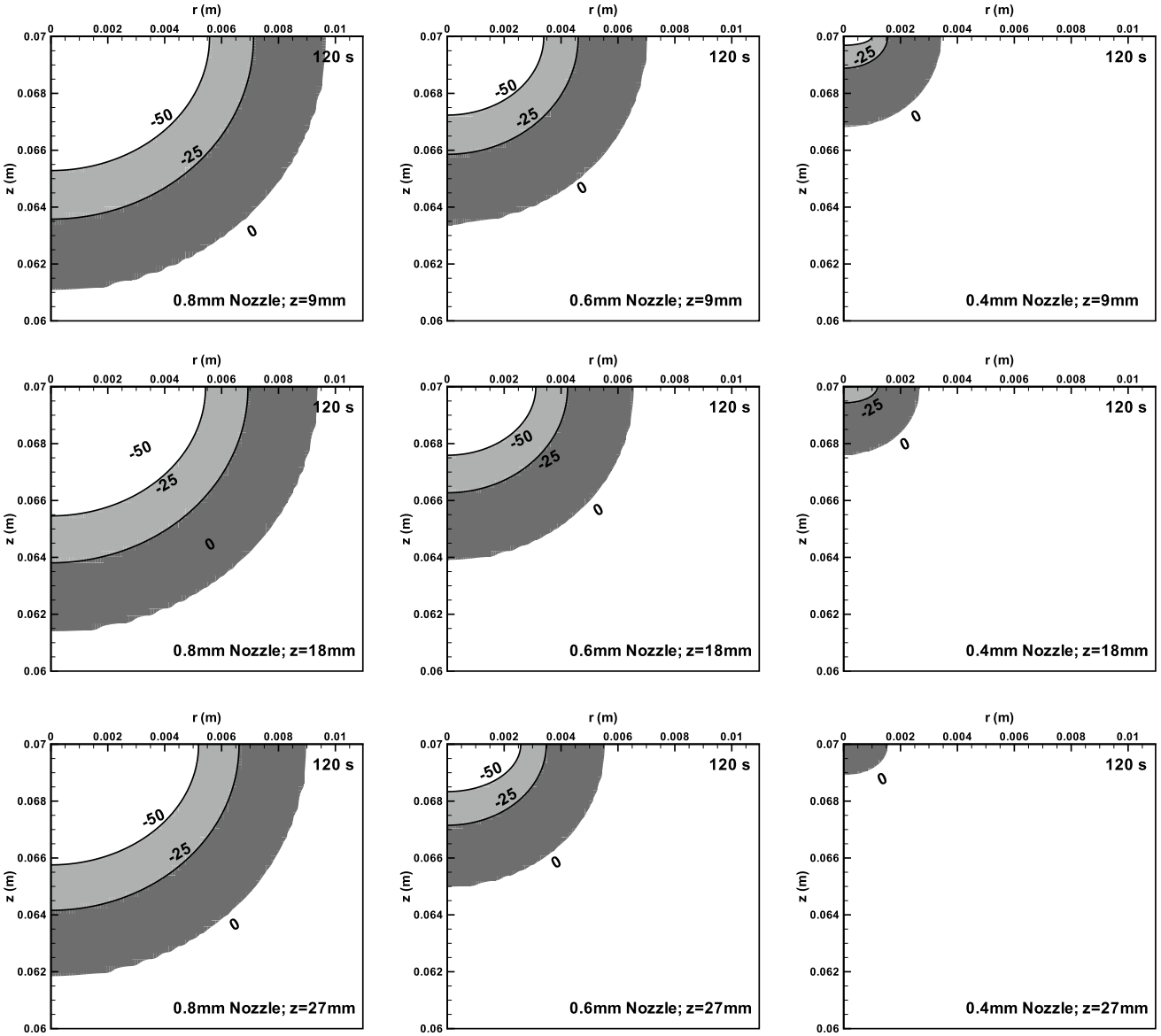

Fig. 10 The − 50 °C, − 25 °C and 0 °C isotherms at 120 s of freezing in a gel model. The lethal isotherms are obtained using various nozzle diameter such as 0.8 mm, 0.6 mm and 0.4 mm nozzle diameter. For each nozzle diameter, the spraying distance is varied as 27 mm, 18 mm and 9 mm

cooling as reported in an earlier study [2]. The necrotic zone characterised by −50 °C and −25 °C isothermal surfaces is substantially higher in the case of 0.8 mm nozzle diameter with spraying distance of 27–9 mm as compared with 0.6 mm nozzle diameter. A similar trend could be observed in terms of heat flux and heat transfer coefficient during cryogen spray cooling with wider and narrow nozzle. Wider nozzle produces coarser spray as compared to the narrow nozzle [1]. In addition to this, the final ablation volume obtained with 0.6 mm nozzle diameter for spraying distance of 27 mm is smaller as compared to 18 mm and 9 mm unlike 0.8 mm nozzle diameter. Furthermore, 0.4 mm nozzle diameter with spraying distance of $z = 9$ mm has a larger ablation volume enclosed by −25 °C isothermal surface. Thus, liquid nitrogen spray with 0.8 mm, 0.6 mm and 0.4 mm nozzle diameters can effectively be used for eradication of skin lesion when the distance from the nozzle to the target site is up to 27 mm, 18 mm and 9 mm respectively. In previous studies, it is reported that liquid nitrogen spray cooling is effective for the treatment of tumours using nozzle size of $C = 0.55$ mm and $B = 0.78$ mm for a spraying distance of 10–20 mm [4, 16, 36]. From the present study, it is suggested that 0.8 mm nozzle diameter is effective for the treatment of a malignant and benign tumour while 0.6 mm nozzle diameter is effective for

Table 4 The optimised spray parameters for the application of skin tumour ablation

Nozzle diameter (mm)	Spraying distance (mm)	Type of tumour
0.8	27	Malignant and benign
0.6	18	Benign
0.4	9	Smaller skin lesions

the treatment of a benign tumour which is also illustrated in Table 4. A similar observation is made for axial and lateral ice front propagation in the gel phantom as shown in Fig. 9. The rate of ice front propagation is larger than ablation volume while comparing nozzle diameter of 0.8 mm and 0.6 mm for 120 s of freezing.

From Fig. 10, it is inferred that cryotherapy with 0.8 nozzle diameter is suitable for malignant lesions of (depth $\leq$ 4.6 mm and diameter $\leq$ 11 mm) and benign lesions of (depth $\leq$ 6.5 mm and diameter $\leq$ 14.2 mm), as calculated from the numerical study. In the same context, 0.6 mm nozzle diameter is effective for benign lesions of (depth $\leq$ 4.1 mm and diameter $\leq$ 9 mm) while 0.4 mm nozzle diameter for smaller skin lesions of (depth $\leq$ 1 mm and diameter $\leq$ 3 mm). The rate of increment of killing zone is lesser with an increase in spraying distance as compared to the ice zone for each nozzle diameter. In addition, the region of gap (the difference between lethal and ice front) remains approximately same for each spraying distance with 0.8 mm and 0.6 mm nozzle diameters. In a recent study, it is reported that the open spray technique is effective for skin lesions less than 20 mm in diameter and 3 mm in depth [39]. However, the data obtained from the present results suggest that the maximum depth of 6.5 mm and 4.6 mm can be effectively used to treat benign and malignant lesion respectively with the suggested spray parameters. The similar figures for the maximum diameter are 14.2 mm and 11 mm for the treatment of benign and malignant tumour respectively.

During cryogen spray cooling, the heat sink in the skin is mainly affected by the thermal properties of tissue, blood perfusion and metabolic heat generation. The blood perfusion and metabolic heat generation lead to decrease in the ice front propagation as compared to the absence of this in the tissue model. However, these terms are neglected while solving the numerical equation because the experiment is performed on the tissue mimicking gel. Although, the present study gives a direction to the dermatologist but it cannot be used on patients yet. Hence, the thermal analysis must be conducted on in-vivo study in order to obtain precise values before proceeding for clinical application.

Conclusion

From the experimental and numerical results obtained in this study, we found out that

1. The numerically calculated data matches well with the experimentally measured data for in-vitro study.
2. Correlations exist between ablation volume and ice front propagation in radial and axial directions, which are valid for freeze duration of 120 s, nozzle diameter of 0.8 mm, 0.6 mm and 0.4 mm and spraying distance of 27 mm, 18 mm and 9 mm.
3. The nozzle diameter has a higher impact on ablation volume as compared to spraying distance.
4. The nozzle diameter of 0.8 mm, 0.6 mm and 0.4 mm is effective with the spraying distance up to 27 mm, 18 mm and 9 mm respectively.
5. Liquid nitrogen spray cooling with the nozzle diameter of 0.8 mm, 0.6 mm and 0.4 mm is suitable for skin tumours with maximum diameter and depth of 14.2 mm, 6.5 mm, 9 mm, 4.1 mm and 3 mm, 1 mm respectively.

Compliance with ethical standards

Conflict of interest The authors declare that they have no conflict of interest.

Ethical approval This article does not contain any studies with human participants or animals performed by any of the authors.

References

1. Aguilar G, Majaron V, Verkruysse W (2001) Theoretical and experimental analysis of droplet diameter, temperature and evaporation rate evolution in cryogenic sprays. Int J Heat Mass Transf 44:3201–3211
2. Aguilar G, Majaron B, Karapetian E (2003) Experimental study of cryogen spray properties for application in dermatologic laser surgery. IEEE Trans Biomed Eng 50:863–869
3. Allington HV (1950) Liquid nitrogen in the treatment of skin diseases. Calif Med 72:153–155
4. Andrews M (2004) Cryosurgery for common skin conditions. Am Fam Phys 69:2365–2372
5. Beckerman G, Shitzer A, Degani D (2009) Numerical simulation of the effects of a thermally significant blood vessel on a freezing by a circular surface cryosurgical probe compared with experimental data. J Heat Transf 131:1–9
6. Bischof JC, Hoffmann NE (2001) Cryosurgery of normal and tumor tissue in the dorsal skin flap chamber: part I-thermal response. ASME J Biomech Eng 123:301–309
7. Breitbart EW (1990) Cryosurgery in the treatment of cutaneous malignant melanoma. Clin Dermatol 8:96–100
8. Budman H, Dayan J, Shitzer A (1991) Controlled freezing of non-ideal solutions with application to cryosurgical processes. ASME J Biomech Eng 113:430–437

9. Chakraborty PR (2017) Enthalpy porosity model for melting and solidification of pure-substances with large difference in phase specific heats. Int Commun Heat Mass 81:183–189
10. Chua KJ (2011) Computer simulations on multiprobe freezing of irregularly shaped tumors. Comput Biol Med 41:493–505
11. Chua KJ (2013) Fundamental experiments and numerical investigation of cryo-freezing incorporating vascular network with enhanced nano-freezing. Int J Therm Sci 70:17–31
12. Duck FA (1990) Physical properties of tissue. Academic Press Inc., San Diego
13. Ferziger JH, Peric M (2002) Computational methods for fluid dynamics, 3rd edn. Springer, Berlin
14. Ge MY, Shu C, Yang WM, Chua KJ (2017) Incorporating an immersed boundary method to study thermal effects of vascular systems during tissue cryo-freezing. J Therm Biol 64:92–99
15. Hakverdi S, Balci DD, Dogramaci CA, Toprak S, Yaldiz M (2011) Retrospective analysis of basal cell carcinoma. Indian J Dermatol Venereol Leprol 77:1–7
16. Kuflik EG (1994) Cryosurgery updated. J Am Acad Dermatol 31:925–944
17. Kumar A (2014) Cryosurgery of a biological tissue with multiprobe: effect of central cryoprobe. Heat Mass Transf 50:1751–1764
18. Kumari C, Kumar A, Sarangi SK, Thirugnanam A (2018a) Effect of adjuvant on cutaneous cryotherapy. Heat Mass Transf. https://doi.org/10.10007/s00231-018-2407-2
19. Kumari C, Kumar A, Sarangi SK, Thirugnanam A (2018b) An experimental and numerical study on liquid nitrogen spray cooling for cryotherapy. Cryobiology 80:179
20. Kumari C, Kumar A, Sarangi SK, Thirugnanam A (2018c) An experimental and numerical study on nodular gel phantom during cryotherapy. CryoLetters 39:137–146
21. Lung DC, Stahovich TF, Rabin Y (2004) Computerised planning for multiprobe cryosurgery using a force-field analogy. Comput Methods Biomech Biomed Eng 7:101–110
22. Massalha L, Shitzer A (2004) Freezing by a flat, circular surface cryoprobe of a tissue phantom with an embedded cylindrical heat source simulating a blood vessel. ASME J Biomech Eng 126:736–744
23. Mercer GN, Tyson AH (2009) Modelling the cryogenic treatment of warts and recommendations for changes to current practise. ANZIAM 50:976–989
24. Pogrel AM, Yen KC, Taylor R (1996) A study of infrared thermographic assessment of liquid nitrogen cryotherapy. Oral Surg Oral Med Oral Pathol Oral Radiol Endod 81:396–401
25. Rabin Y, Coleman R, Mordohovich D, Ber R, Shitzer A (1996) A new cryosurgical device for controlled freezing ii. in vivo experiments on skeletal muscle of rabbit hindlimbs. Cryobiology 33:93–105
26. Ramajayam KK, Kumar A, Sarangi SK, Thirugnanam A (2016) A novel adjuvant solution layer strategy for improving the efficacy of cryosurgery. CryoLetters 37:346–356
27. Ramajayam KK, Kumar A, Sarangi SK, Thirugnanam A (2017) A numerical study on optimising the cryosurgical process for effective tumour necrosis. Heat Mass Transf 53:1685–1697
28. Rossi MR, Tanaka D, Shimada K, Rabin Y (2008) Computerized planning of cryosurgery using bubble packing: an experimental validation on a phantom material. Int J Heat Mass Transf 51:5671–5678
29. Shepherd JP, Dawber RP (1984) Wound healing and scarring after cryosurgery. Cryobiology 21:157–169
30. Singh S, Kumar S (2014) Numerical study on triple layer skin tissue freezing using dual phase lag bio-heat model. Int J Therm Sci 86:12–20
31. Sun F, Wang GX, Kelly KM, Aguilar G (2005) Numerical modeling of the tissue freeze-thaw cycle during cutaneous cryosurgery using liquid nitrogen spray. 2005 ASME IMECE, Orlando, pp 1–8
32. Sun F, Martinez-Suastegui L, Wang GX, Kelly MK, Aguilar G (2012) Numerical prediction of the intracellular ice formation zone during cryosurgery on a nodular basal cell carcinoma using liquid nitrogen spray. Int J Spray Combust 4:341–380
33. Takeda H, Maruyama S, Okajima J, Aiba S, Komiya A (2009) Development and estimation of a novel cryoprobe utilizing the Peltier effect for precise and safe cryosurgery. Cryobiology 59:275–284
34. Torre D (1979) Understanding the relationship between lateral spread of freeze and depth of freeze. J Dermatol Surg Oncol 5:51–53
35. Tunnel J, Torres JH, Anvari B (2002) Methodology for estimation of time-dependent surface heat flux due to cryogen spray cooling. Ann Biomed Eng 30:19–33
36. Usatine RP, Stulber DL, Colver GB (2005) Cutaneous cryosurgery, 4th edn. Taylor and Francis Group, New York
37. Voller VR, Prakash C (1987) A fixed grid numerical modeling methodology for convection-diffusion mushy region phase-change problems. Int J Heat Mass Transf 30(8):1709–1719
38. Zacarian SA (1978) Cryo corner: is lateral spread of freeze a valid guide to depth of freeze. J Dermatol Surg Oncol 4:561–562
39. Zimmerman EE, Crawford P (2012) Cutaneous cryosurgery. Am Fam Phys 86:1118–1124
40. Zouboulis C (1999) Principles of cutaneous cryosurgery: an update. Dermatology 198:111–117